



Geophysical Research Letters

RESEARCH LETTER

10.1002/2014GL059856

Key Points:

- Mean global permeability is consistent with previous estimates of shallow crust
- The spatially-distributed mean porosity of the globe is 14%
- Maps will enable groundwater in land surface, hydrologic and climate models

Correspondence to:

T. Gleeson,
tom.gleeson@mcgill.ca

Citation:

Gleeson, T., N. Moosdorf, J. Hartmann, and L. P. H. van Beek (2014), A glimpse beneath earth's surface: Global HYdrogeology MaPS (GLHYMPS) of permeability and porosity, *Geophys. Res. Lett.*, 41, 3891–3898, doi:10.1002/2014GL059856.

Received 21 MAR 2014

Accepted 15 MAY 2014

Accepted article online 16 MAY 2014

Published online 9 JUN 2014

A glimpse beneath earth's surface: GLobal HYdrogeology MaPS (GLHYMPS) of permeability and porosity

Tom Gleeson¹, Nils Moosdorf², Jens Hartmann², and L. P. H. van Beek³

¹Department of Civil Engineering, McGill University, Montreal, Quebec, Canada, ²Institute for Geology, Center for Earth System Research and Sustainability, University of Hamburg, Hamburg, Germany, ³Department of Physical Geography, Faculty of Geosciences, Utrecht University, Utrecht, Netherlands

Abstract The lack of robust, spatially distributed subsurface data is the key obstacle limiting the implementation of complex and realistic groundwater dynamics into global land surface, hydrologic, and climate models. We map and analyze permeability and porosity globally and at high resolution for the first time. The new permeability and porosity maps are based on a recently completed high-resolution global lithology map that differentiates fine and coarse-grained sediments and sedimentary rocks, which is important since these have different permeabilities. The average polygon size in the new map is $\sim 100 \text{ km}^2$, which is a more than hundredfold increase in resolution compared to the previous map which has an average polygon size of $\sim 14,000 \text{ km}^2$. We also significantly improve the representation in regions of weathered tropical soils and permafrost. The spatially distributed mean global permeability $\sim 10^{-15} \text{ m}^2$ with permafrost or $\sim 10^{-14} \text{ m}^2$ without permafrost. The spatially distributed mean porosity of the globe is 14%. The maps will enable further integration of groundwater dynamics into land surface, hydrologic, and climate models.

1. Introduction

A number of fundamental and applied scientific problems and policy issues need improved data sets of global hydrogeologic parameters and a better understanding of groundwater systems at regional to continental scales. These problems include the complex coupling between groundwater, climate, and global change [Maxwell and Kollet, 2008; Taylor et al., 2013], global groundwater stress and depletion [Wada et al., 2010; Konikow, 2011; Aeschbach-Hertig and Gleeson, 2012; Döll et al., 2012; Gleeson et al., 2012; Pokhrel et al., 2012], and the role of groundwater in base flow and ecological flows [Smakhtin, 2001; Smakhtin et al., 2004; Poff et al., 2009] and groundwater as a component of blue water in global virtual water modeling and water footprint calculations [Rohwer et al., 2007; Rost et al., 2008; Hoekstra, 2009; Hoff et al., 2010; Hanasaki et al., 2010; Hoekstra and Mekonnen, 2012; Hoekstra et al., 2012]. Groundwater systems have been integrated into some global hydrologic models [i.e., Döll and Fiedler, 2008; Wada et al., 2012]; and the water table has been modeled globally [Fan et al., 2013], but the dynamic nature of the water table has not been explicitly incorporated into these models and lateral groundwater flow has only been simulated using soil permeability [Krakauer et al., 2014]. The lack of robust, spatially distributed subsurface data is one of the primary reasons why more complex and realistic groundwater dynamics are not integrated into global hydrologic models, with current attempts limiting themselves to regional applications in data-rich locations [Sutanudjaja et al., 2011; Vergnes et al., 2012].

Two of the most important hydrogeologic parameters are permeability and porosity. Permeability, the ease of fluid flow through porous media, is a fundamental control on subsurface flow at all depths. Porosity, a measure of the void spaces in a material, controls how much water can be stored in the subsurface. Global hydrologic models that include groundwater generally use permeability and porosity of the soil, which only represents the first couple of meters of the subsurface. However, the deeper subsoil permeability is essential to constrain and quantify the water table dynamics and lateral/regional groundwater flow, especially in arid or mountainous regions with deeper water tables. The deeper, subsoil permeability, mapped globally at a coarse resolution by Gleeson et al. [2011], is starting to be incorporated in regional to global hydrologic models. Previous efforts have synthesized hydrogeologic parameters at the continental to global scale [U.S. Geological Survey, 2003; Bundesanstalt für Geowissenschaften und Rohstoffe/United Nations Educational, Scientific and Cultural Organization (BGR/UNESCO), 2008; Gleeson et al., 2011; MacDonald et al., 2012]. For example, Figure 1 illustrates

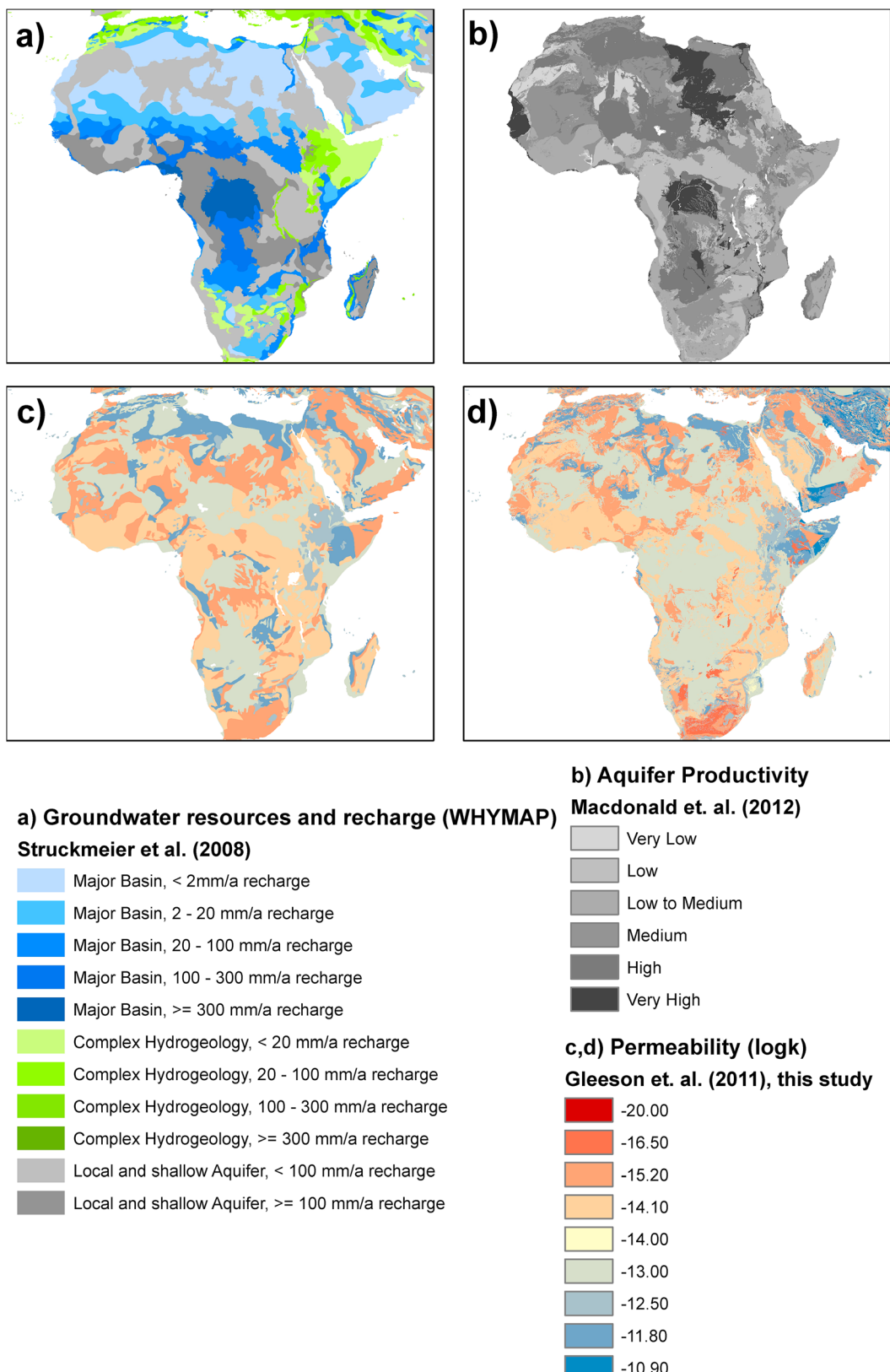


Figure 1. Examples of previous efforts that have synthesized hydrogeologic parameters at the continental to global scale for Africa including (a) groundwater resources and recharge [BGR/UNESCO, 2008], (b) aquifer productivity [MacDonald et al., 2012], (c) coarse-resolution permeability [Gleeson et al., 2011], and (d) high-resolution permeability (this study).

Table 1. Hydrolithological and Lithological Categories [After Gleeson *et al.*, 2011]^a

Hydrolithology	Permeability $\log(k) \mu_{\text{geo}}$ (m^2)	Permeability $\log(k) \sigma$ (m^2)	Porosity	Lithology ^b	Sublithology ^b
Unconsolidated	-13.0	2.0	0.22	SU, WB	
c.g. unconsolidated	-10.9	1.2	0.28	SU	SS
f.g. unconsolidated	-14.0	1.8	0.15	SU	SH
sil. Sedimentary	-15.2	2.5	0.19	SS, SM	
c.g. sil. Sedimentary	-12.5	0.9	0.27	SS, SM	SS
f.g. sil. Sedimentary	-16.5	1.7	0.12	SS, SM, EV	SH
Carbonate	-11.8	1.5	0.06	SC	
Crystalline	-14.1	1.5	0.01	MT, PA, PB, PI	
Volcanic	-12.5	1.8	0.09	VA, VB, VI, PY	
Not assigned	-20 (-)	-	-	ND, IG	

^a $\log k \mu_{\text{geo}}$ is the geometric mean logarithmic permeability; σ is the standard deviation; n is the number of hydrolithologic units; sil. sedimentary is siliciclastic sedimentary; c.g. and f.g. are coarse grained and fine grained, respectively.

^b Lithology and sublithology codes from [Hartmann and Moosdorf, 2012]. If no sublithology is provided, all sublithology classes except those explicitly mentioned in other lines are included in the definition.

how aquifer productivity for Africa [MacDonald *et al.*, 2012] compares to global coarse resolution mapping of groundwater resources and recharge [BGR/UNESCO, 2008], and permeability [Gleeson *et al.*, 2011].

Our objective is to map and analyze permeability and porosity globally and at high resolution for the first time. We expect our spatially distributed data will be useful for a number of fundamental and applied scientific problems and policy issues. Specifically, we hope the new data will enable further integration of groundwater dynamics into land surface, hydrologic, and climate models. The new permeability map is based on a recently completed high-resolution global lithology map [Hartmann and Moosdorf, 2012] with important refinements in regions of weathered tropical soils and permafrost regions. Together these new, freely available maps of permeability and porosity are called the GLobal HYdrogeology MaPS (GLHYMPS).

2. Methodology

This study derives new maps of near-surface permeability and porosity by synthesizing and modifying existing global databases into new databases. Gleeson *et al.* [2011] previously compiled 233 hydrogeologic units from calibrated groundwater models of diverse hydrogeologic conditions in North America (Arizona (6 hydrogeologic units), British Columbia (1), California (4), Florida (4), Georgia (1), Manitoba (7), Massachusetts (2), Minnesota (3), Mississippi (26), Nevada (119), New Mexico (15), Ontario (16), Oregon (1), South Carolina (1), South Dakota (2), Southeastern USA (26), Texas (1), Utah (2), Virginia (19), and Wisconsin (1)) and around the world (Argentina (1), Bangladesh (2), Barbados (1), Belgium (6), Brazil (1), Chile (1), China (2), Finland (1), France (2), India (3), Nicaragua (8), Poland (5), Switzerland (1), and Vietnam (4); see supporting information of Gleeson *et al.* [2011] for full data set and description of methodology). Only peer-reviewed, calibrated models with hydrolithologic units that are >5 km in length with a shallow upper contact (<100 m depth) were included. The minimum length scale was set to be above the scale at which heterogeneities such as discrete fractures control groundwater flow. Potential bias is reduced by including a diversity of model software, modelers, geographical areas and calibration targets (flow, tracer, and heat), and excluding multiple models from the same geographic area. Data were grouped into five hydrolithologic categories: unconsolidated sediments, siliciclastic sedimentary, carbonate, crystalline, and volcanic (Table 1). Unconsolidated sediments and siliciclastic sedimentary were further divided into fine grained and coarse grained. Although this compilation is biased toward North America, Gleeson *et al.* [2011] found that the logarithmic permeability of each hydrology is normally distributed, scale independent at these regional scales, and best described using the geometric mean. Using these seven hydrolithologic categories, near-surface permeability was mapped globally at low resolution and for North America at high resolution by pairing the geometric mean permeability values of each hydrolithogey with the polygons of a lithology map [Dürr *et al.*, 2005; Moosdorf *et al.*, 2010]. The previous global permeability map had four significant limitations: (1) the resolution was coarse; (2) unconsolidated sediments and siliciclastic sedimentary could not be divided into fine grained and coarse grained so the combined permeability values with larger uncertainties had to be used for these categories; (3) the very low permeability of frozen ground [Freeze and Cherry, 1979] was not represented; and (4) in tropical regions the bedrock lithology mapped on the surface may in fact be deeply weathered

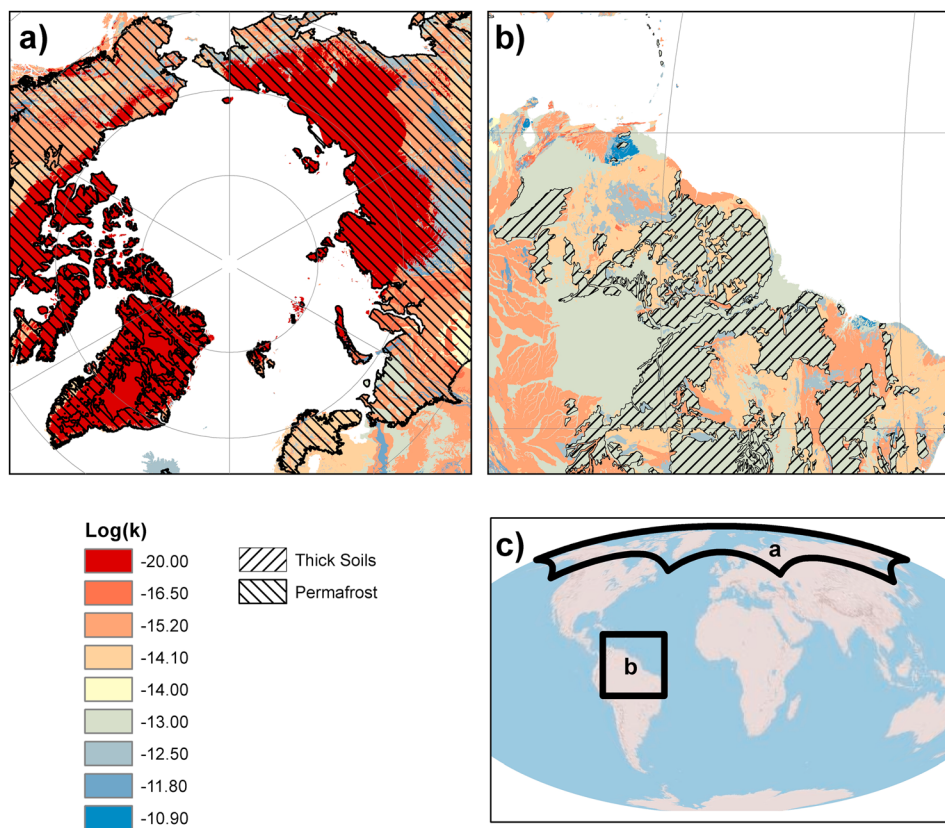


Figure 2. Detail to show the modifications made to the permeability map of (a) an Arctic region for permafrost and (b) a tropical region for weathering. (c) The extent of Figures 2a and 2b.

laterite, which was also not represented. The high-resolution map of North America had an additional limitation of artifacts at some jurisdictional boundaries due to different data sources.

First, the previously derived permeability values (Table 1) are combined with a higher-resolution global lithology map (GLiM) [Hartmann and Moosdorf, 2012] and then modified to address the previous limitations in the global map. GLiM was assembled and translated from 92 regional geological maps and consists of a total of 1,200,000 polygons representing geological units. The “average” scale of the GLiM is 1:3,750,000 [Hartmann and Moosdorf, 2012]. The global lithology maps do not include geological structures such as fault zones. Following Gleeson *et al.* [2011], we adopt the geometric mean as the best and scale-independent estimate of regional-scale permeability.

Second, unconsolidated and consolidated siliciclastic-dominated sediment rock lithologies were mapped in greater detail in GLiM so that they could often be divided into fine grained, coarse grained, or characterized as mixed (i.e., without a dominant grain size). Characteristics of sedimentary units were examined during translation of geological maps instead of just focusing on their stratigraphic age. In sum, the sedimentary classes represent 6100 different rock descriptions, ranging in detail from “sediment, undifferentiated” to “cross bedded and rippled medium to fine-grained quartz sandstone with shale pellet layers in places; minor shale, siltstone, limestone and chert with conglomerate and sublithic sandstone near the base.” Analysis of the individual rock descriptions shows that the geological features are often finer than the assessed scale; and thus, a minority of units is consistently fine or coarse grained in the GLiM database.

Third, the GLiM was merged with spatial information on permafrost using the permafrost zonation index (PZI) [Gruber, 2012]. In areas with continuous permafrost (defined at PZI > 0.99), the permeability was assigned a value of $\log(k) = -20$, assuming that the ice prohibits groundwater flow (Figure 2a). Permeability values are not reassigned in regions of discontinuous permafrost due to the unknown relationship between PZI and permeability, but the maximum expectable permafrost extent ($PZI > 0$) is shown in Figures 2a and 3a for reference. The new global permeability map is available with or without the permafrost reassignment so that it can be used in climate change analysis.

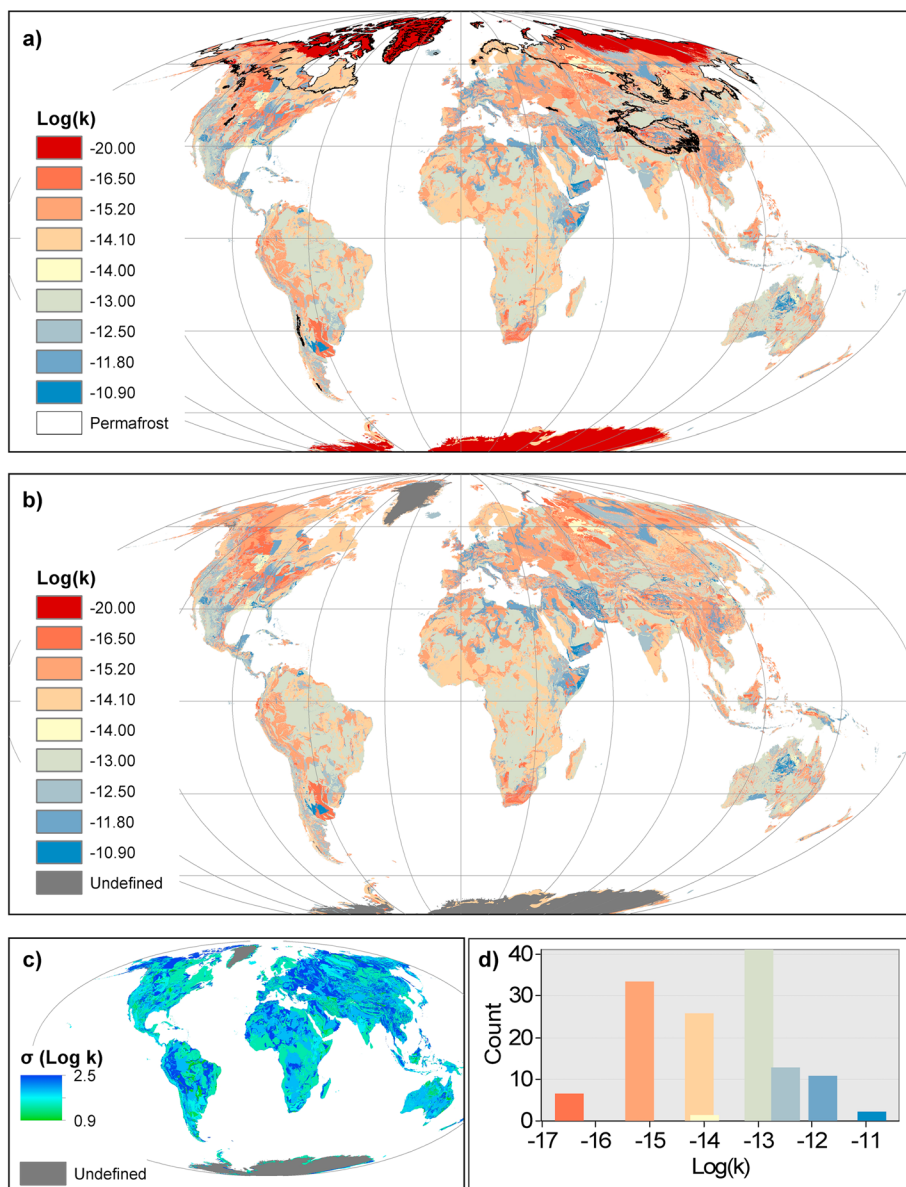


Figure 3. New global high-resolution maps of near-surface permeability. (a) Global map with permeability with regions of continuous permafrost set to $\log(k) = -20$ and (b) with permeability unaffected by continuous permafrost. The maximum permafrost extent is also shown from Gruber [2012]. (c) The uncertainty of permeability as shown by the standard deviation of the geometric mean (Table 1). (d) Histogram of the logarithmic permeability of ice-free areas neglecting permafrost effects (Figure 3b). The average polygon size in the new map is 107 km^2 (including Antarctica) compared to the previous map based on Dürr *et al.* [2005], which has an average polygon size of $14,000 \text{ km}^2$.

Fourth, the GLIM was refined in regions of deeply weathered soils (“laterite” soil class in *Food and Agriculture Organization* [2009]). In these regions, the permeability value is likely dominated by the soil and not by the bedrock tens of meters below the surface. Thus, areas with mapped laterite in the World Harmonized Soil Database were assigned the permeability value of unconsolidated sediment hydrogeologies (Table 1). Figure 2b shows how the deeply weathered soils in the Amazon basin were remapped as an example.

Finally, porosity values from literature (Table 1) are combined with the higher-resolution lithology map in a similar way as the permeability values. Porosity or storage coefficient is defined as the fraction of the volume of voids over the total volume and derived from Morris and Johnson [1967] and Rasmussen [1963]. Deeply weathered soils in tropical regions were treated as mixed unconsolidated sediments.

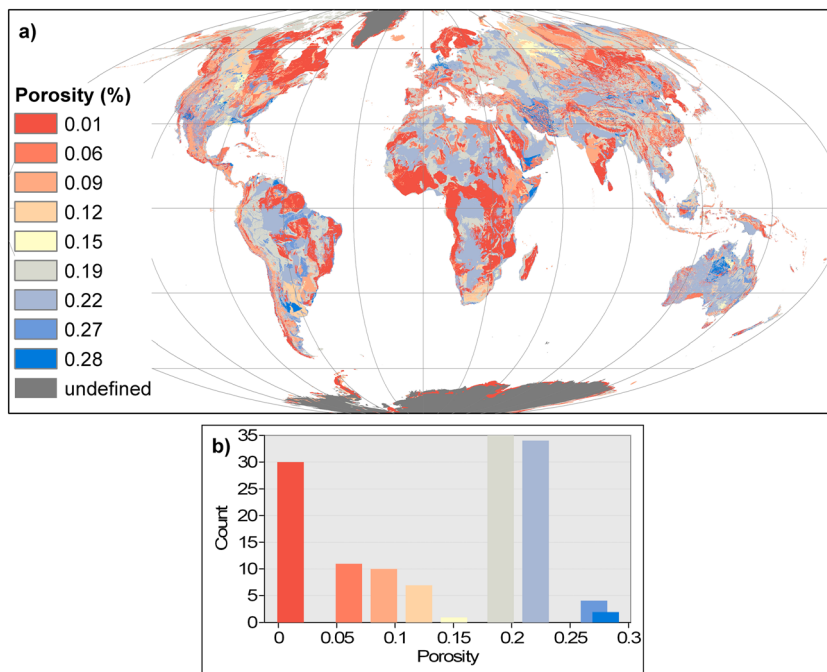


Figure 4. New global high-resolution map of near-surface porosity and histogram.

3. Results and Conclusions

Figure 3 shows the new global high-resolution map of near-surface permeability either with regions of continuous permafrost set to very low permeability (Figure 3a), or assuming permafrost does not modify the permeability (Figure 3b). The permeability map has an inherent uncertainty represented by the standard deviation of the individual hydrolithologies which is mapped globally in Figure 3c. The spatially distributed mean logarithmic permeabilities [$\log(k)$] for the globe (assuming permafrost regions have very low permeability [$\log(k) = -20$] and excluding glaciated regions) is $-14.56 \pm 1.9 \text{ m}^2$. This spatially distributed mean permeability is consistent with previous estimates of shallow crustal permeability [Ingebritsen and Manning, 1999; Gleeson *et al.*, 2011]. The spatially distributed mean logarithmic permeability for a world without permafrost is -13.77 m^2 . Porosity values from literature (Table 1) are combined with the higher-resolution lithology map in a similar way as the permeability values in Figure 4. The spatially distributed mean porosity or storage coefficient for the globe is 14%. The average polygon size in the new maps is 107 km^2 (including Antarctica) compared to the previous map based on Dürr *et al.* [2005], which has an average polygon size of $14,000 \text{ km}^2$.

Depending on the application of the permeability maps, various caveats may be important. First, artifacts are present at some jurisdictional boundaries due to different data sources in the global lithological map (GLIM). Although the previous coarse-scale permeability map did not have artifacts at jurisdictional boundaries, the dramatic increase in resolution should outweigh this disadvantage. Second, we focus on saturated permeability, but unsaturated permeabilities that can be much lower than saturated permeabilities are transient and nonlinear depending on lithology and water saturation. To use these permeability maps in Earth system models of regions where unsaturated zone processes are predominant, the relative permeability or constitutive relations between pressure and saturation [e.g., Brooks and Corey, 1964; van Genuchten, 1980] must also be defined. Third, the depths that the permeability maps represent are connected to the depths for which the surface lithologic condition represents the subsurface. We follow Gleeson *et al.* [2011] in estimating that the lithology maps represent the shallow subsurface (on the order of 100 m) as an estimate, although regionally this value may vary strongly. Fourth, the compiled permeability is all regional scale ($>5 \text{ km}$ horizontal distance) and well above the scale at which heterogeneities such as discrete fractures control groundwater flow. Effects of fault zones on the permeability are therefore not included.

A number of fundamental and applied scientific problems and policy issues need improved data sets of global hydrogeologic parameters and a better understanding of groundwater systems at regional to continental scales. We map and analyze permeability and porosity globally and at high resolution for the first time. We expect our spatially distributed data will be useful for a number of fundamental and applied scientific problems and policy issues. These new, freely available maps of permeability and porosity are called the GLHYMPS, which we hope will be useful for a number of fundamental and applied scientific problems and policy issues, especially the integration of groundwater dynamics into land surface, hydrologic, and climate models.

Acknowledgments

All data discussed in this article are freely available by contacting the corresponding author. Tom Gleeson is funded by NSERC, and Nils Moosdorff and Jens Hartmann are funded by the DFG Cluster of Excellence "CliSAP" (EXC177). We thank two anonymous reviewers for suggestions that improved the manuscript.

The Editor thanks two anonymous reviewers for their assistance in evaluating this paper.

References

- Aeschbach-Hertig, W., and T. Gleeson (2012), Regional strategies for the accelerating global problem of groundwater depletion, *Nat. Geosci.*, 5(12), 853–861.
- Brooks, R. H., and A. T. Corey (1964), *Hydraulic Properties of Porous Media*, Hydrology Paper 3, Univ. of Colorado, Fort Collins.
- Bundesanstalt für Geowissenschaften und Rohstoffe/United Nations Educational, Scientific and Cultural Organization (BGR/UNESCO) (2008), Groundwater resources of the world 1:25 000 000.
- Döll, P., and K. Fiedler (2008), Global-scale modeling of groundwater recharge, *Hydrol. Earth Syst. Sci.*, 12, 863–885.
- Döll, P., H. Hoffmann-Dobrev, F. T. Portmann, S. Siebert, A. Eicker, M. Rodell, G. Strassberg, and B. R. Scanlon (2012), Impact of water withdrawals from groundwater and surface water on continental water storage variations, *J. Geodyn.*, 59–60, 143–156.
- Dürr, H. H., M. Meybeck, and S. H. Dürr (2005), Lithologic composition of the Earth's continental surfaces derived from a new digital map emphasizing riverine material transfer, *Global Biogeochem. Cycles*, 19, GB4510, doi:10.1029/2005GB002515.
- Fan, Y., H. Li, and G. Miguez-Macho (2013), Global patterns of groundwater table depth, *Science*, 339(6122), 940–943.
- Food and Agriculture Organization, IASA, ISRIC, ISSCAS, JRC (2009), Harmonized World Soil Database (version 1.1), *Rep. Freeze, R. A., and J. A. Cherry (1979)*, *Groundwater*, 604 pp., Prentice-Hall Inc., Eaglewood Cliffs, N. J.
- Gleeson, T., L. Smith, N. Moosdorff, J. Hartmann, H. H. Dürr, A. H. Manning, L. P. H. van Beek, and A. M. Jellinek (2011), Mapping permeability over the surface of the Earth, *Geophys. Res. Lett.*, 38, L02401, doi:10.1029/2010GL045565.
- Gleeson, T., Y. Wada, M. F. P. Bierkens, and L. P. H. van Beek (2012), Water balance of global aquifers revealed by groundwater footprint, *Nature*, 488(7410), 197–200.
- Gruber, S. (2012), Derivation and analysis of a high-resolution estimate of global permafrost zonation, *Cryosphere*, 6, 221–233.
- Hanasaki, N., T. Inuzuka, S. Kanae, and T. Oki (2010), An estimation of global virtual water flow and sources of water withdrawal for major crops and livestock products using a global hydrological model, *J. Hydrol.*, 384(3–4), 232–244.
- Hartmann, J., and N. Moosdorff (2012), The new global lithological map database GLIM: A representation of rock properties at the Earth surface, *Geochem. Geophys. Geosyst.*, 13, Q12004, doi:10.1029/2012GC004370.
- Hoekstra, A. Y. (2009), Human appropriation of natural capital: A comparison of ecological footprint and water footprint analysis, *Ecol. Econ.*, 68(7), 1963–1974.
- Hoekstra, A. Y., and M. M. Mekonnen (2012), The water footprint of humanity, *Proc. Natl. Acad. Sci. U.S.A.*, 109, 3232–3237, doi:10.1073/pnas.1109936109.
- Hoekstra, A. Y., M. M. Mekonnen, A. K. Chapagain, R. E. Mathews, and B. D. Richter (2012), Global monthly water scarcity: Blue water footprints versus blue water availability, *PLoS One*, 7(2), e32688.
- Hoff, H., M. Falkenmark, D. Gerten, L. Gordon, L. Karlberg, and J. Rockström (2010), Greening the global water system, *J. Hydrol.*, 384(3–4), 177–186.
- Ingebritsen, S. E., and C. E. Manning (1999), Geological implications of a permeability-depth curve for the continental crust, *Geology*, 27(12), 1107–1110.
- Konikow, L. F. (2011), Contribution of global groundwater depletion since 1900 to sea-level rise, *Geophys. Res. Lett.*, 38, L17401, doi:10.1029/2011GL048604.
- Krakauer, N. Y., H. Li, and Y. Fan (2014), Groundwater flow across spatial scales: Importance for climate modeling, *Environ. Res. Lett.*, 9(3), 034003.
- MacDonald, A. M., H. C. Bonsor, B. É. Dochartaigh, and R. G. Taylor (2012), Quantitative maps of groundwater resources in Africa, *Environ. Res. Lett.*, 7(2), 024,009.
- Maxwell, R. M., and S. J. Kollet (2008), Interdependence of groundwater dynamics and land-energy feedbacks under climate change, *Nat. Geosci.*, 1(10), 665–669.
- Moosdorff, N., J. Hartmann, and H. H. Dürr (2010), Lithological composition of the North American continent and implications of lithological map resolution for dissolved silica flux modeling, *Geochem. Geophys. Geosyst.*, 11, Q11003, doi:10.1029/2010GC003259.
- Morris, D. A., and A. I. Johnson (1967), Summary of hydrologic and physical properties of rock and soil materials as analyzed by the Hydrologic Laboratory of the U.S. Geological Survey, U.S. Geol. Surv. Water-Supply Paper 1839-D^{Rep.}, 42 pp.
- Poff, N. L., et al. (2009), The ecological limits of hydrologic alteration (ELOHA): A new framework for developing regional environmental flow standards, *Freshwater Biol.*, 55(1), 147–170.
- Pokhrel, Y. N., N. Hanasaki, P. J. F. Yeh, T. J. Yamada, S. Kanae, and T. Oki (2012), Model estimates of sea-level change due to anthropogenic impacts on terrestrial water storage, *Nat. Geosci.*, 5(6), 389–392.
- Rasmussen, W. C. (1963), Permeability and storage of heterogeneous aquifers in the United States, International union of geodesy and geophysics, Berkeley, August.
- Rohwer, J., D. Gerten, and W. Lucht (2007), Development of functional types of irrigation for improved global crop modelling, *PIK Report 104*, Potsdam Institute for Climate Impact Research, Potsdam, Germany.
- Rost, S., D. Gerten, A. Bondeau, W. Lucht, J. Rohwer, and S. Schaphoff (2008), Agricultural green and blue water consumption and its influence on the global water system, *Water Resour. Res.*, 44, W09405, doi:10.1029/2007WR006331.
- Smakhtin, V. U. (2001), Low flow hydrology: A review, *J. Hydrol.*, 240, 147–186.
- Smakhtin, V. U., C. Revenga, and P. Döll (2004), A pilot global assessment of environmental water requirements and scarcity, *Water Int.*, 29(3), 307–317.

- Sutanudjaja, E. H., L. P. H. van Beek, S. M. de Jong, F. C. van Geer, and M. F. P. Bierkens (2011), Large-scale groundwater modeling using global datasets: A test case for the Rhine-Meuse basin, *Hydrol. Earth Syst. Sci. Discuss.*, 8(2), 2555–2608.
- Taylor, R. G., et al. (2013), Ground water and climate change, *Nat. Clim. Change*, 3(4), 322–329.
- U.S. Geological Survey (2003), Principal aquifers of the 48 conterminous United States, Hawaii, Puerto Rico, and the U.S. Virgin Islands, *Rep. van Genuchten*, M. T. (1980), A closed-form equation for predicting the hydraulic conductivity of unsaturated soils, *Soil Sci. Soc. Am. J.*, 24(2), 133–144.
- Vergnes, J. P., B. Decharme, R. Alkama, E. Martin, F. Habets, and H. Douville (2012), A simple groundwater scheme for hydrological and climate applications: Description and offline evaluation over France, *J. Hydrometeorol.*, 13(4), 1149–1171.
- Wada, Y., L. P. H. van Beek, C. M. van Kempen, J. W. T. M. Reckman, S. Vasak, and M. F. P. Bierkens (2010), Global depletion of groundwater resources, *Geophys. Res. Lett.*, 37, L20402, doi:10.1029/2010GL044571.
- Wada, Y., L. P. H. van Beek, and M. F. P. Bierkens (2012), Nonsustainable groundwater sustaining irrigation: A global assessment, *Water Resour. Res.*, 48, W00L06, doi:10.1029/2011WR010562.